thermo scientific

WHITE PAPER WP53197

Back illuminated vs. front illuminated CCD-based imaging sensors and how it impacts Raman spectra

Author

Robert Heintz

Key Words

CCD, charge-coupled device, EM-CCD, electron multiplied charge-coupled device, front illuminated, back illuminated, Raman spectroscopy, fringing, quantum efficiency, DXR3 Raman Microscope, DXR3xi Raman Imaging Microscope

Introduction

Successful Raman spectroscopy depends on detecting the weak inelastic scattering from a sample. CCD (charge couple device) and EM-CCD (electron multiplied charge couple device) based imaging sensors are popular choices for detecting the Raman scattered light in dispersive Raman spectrometers. The efficiency of this photon-to-signal conversion is based on the design of the CCD sensor. One of the variabilities in CCD design is whether the incident photons impinge on the front side of the sensor (front illuminated) or impinge on the backside of the sensor (back illuminated). This paper will address the advantages and disadvantages of these two sensor designs as it relates to Raman spectroscopy.

Background

CCD based imaging sensors rely on a photoactive (metal oxide semiconductor capacitor) region of the sensor, also known as the depletion region, to convert photons to electron charge. Shorter wavelengths of light are absorbed close to the surface while longer wavelengths travel deeper before being absorbed. If the wavelengths of light are long enough (>1050 nm) they do not interact with the depletion region and do not produce a signal. This is why silicon CCD sensors are not useful detectors for Raman spectroscopy using long wavelength near infrared lasers. The conversion rate of incident photons to electron charge is known as the quantum efficiency (QE). The higher the QE, the greater the signal a given number of photons produces. If noise is assumed to be constant, detectors with higher QE will produce Raman spectra with higher signal-to-noise (S/N) values.

As the electron charge is produced it is held in a series of potential wells (bins or pixels) by gate electrodes. These electrodes transfer the charge from well to well. In this way the charge can be collected in discrete wells and then moved systematically to a read-out row where the charge (signal) in each well is measured. When the Raman scatter is dispersed by wavelength across the pixels of a CCD and then each pixel is read individually, the results can be compiled to construct the Raman spectrum. We have written a separate paper comparing CCDs and EM-CCDs; here, CCD will be used collectively except when a specific difference needs to be specified.[1]

ThermoFisher SCIENTIFIC

The differences between front illuminated and back illuminated CCD imaging sensors arise from the way the incident photons get to the photoactive region of the sensor. A simple schematic of a front illuminated CCD detector is shown in Figure 1. As shown, the photons impinge on the same side of the device as the gate electrodes (hence, the front). In this design, the gate electrodes can absorb or reflect some of the photons and thus limit the number of photons that actually reach the photosensitive region. Since fewer photons get to the photosensitive region this typically limits the QE to around 50–60%.

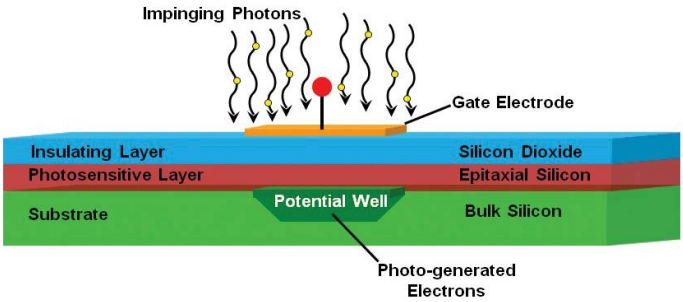

Figure 1: Schematic representation of a front illuminated CCD device.

Alternately, the photons can arrive through the back of the sensor (hence, back illuminated). In order to make this work effectively it is necessary to remove, mechanically or via chemical etching, some of the bulk silicon substrate to provide access to the photoactive region (Figure 2). This is why these types of CCD sensors are also known as back thinned devices. Back illuminated CCDs can attain QEs up to 95%.

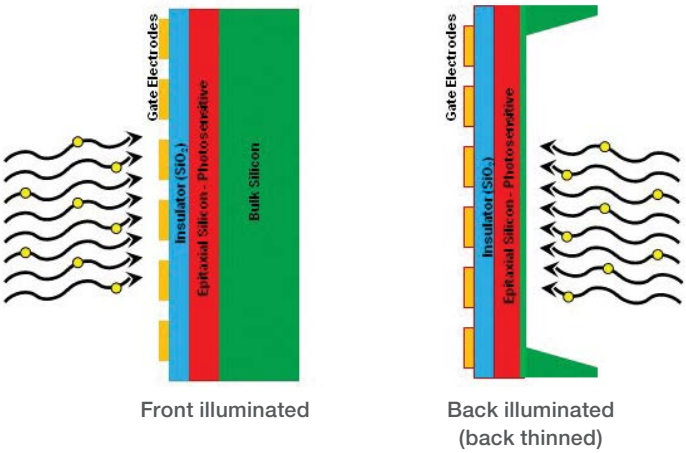

Figure 2: Front versus back illuminated geometry for a CCD sensor.

The higher QE of back illuminated CCDs would appear to provide a clear advantage. However, there is a drawback. As noted, longer wavelengths of light penetrate much further in the silicon. This longer penetration can result in the long wavelength of light passing all the way through the photosensitive region and reflecting off the surfaces to create an étalon type structure (see Figure 3). This can lead to interference fringes superimposed on the normal Raman spectrum. The fringing sharpness and amplitude depends on the optical qualities of the étalon structure and on the wavelength and intensity of the photons involved.

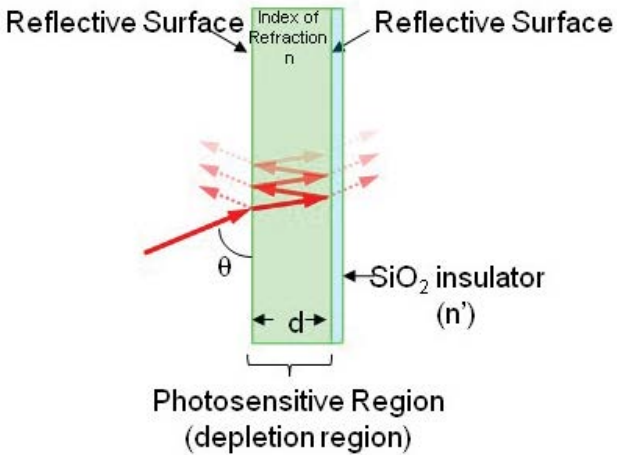

Figure 3: Étalon structure created by deep penetration of long wavelength light through the depletion region and reflections from the boundary surfaces. Internal reflections and interferences result in the fringing effects seen in Raman spectra.

Two types of étaloning can be observed with back illuminated CCDs. The first type is known as spatial étaloning which results from very slight differences in the thickness of the layers in a CCD. This type of étaloning can be used to visualize the uniformity of the CCD itself. The other type of étaloning is known as spectroscopic étaloning and is caused by variations of the wavelengths of light across the CCD. Both types of étaloning can produce spectral artifacts.

Approaches like deep depletion (increasing the thickness of the photo-sensitive area) have proved useful for CCDs but have yet to be realized commercially for EM-CCDs. Anti-reflection coatings and “fringe-suppression” approaches such as controlled roughening of surfaces in the EM-CCDs can suppress, but not entirely remove, these effects. We will use some examples to show how the étaloning affects the Raman spectra of different types of samples.

Experimental

Raman imaging data and some of the individual spectra shown here were collected using a Thermo Scientific™ DXR3xi Raman Imaging Microscope with either a back illuminated EM-CCD detector with fringe suppression or a front illuminated EM-CCD detector,

as noted. Raman spectra were also collected using a Thermo Scientific™ DXR3 Raman Microscope equipped with a front illuminated CCD detector. Lasers with emissions at 532, 780 nm, and 785 nm were used to demonstrate the presence or absence of fringing and the QE qualities of the various detectors.

Results

The effects of fringing are most apparent in samples with significant fluorescence contributions. The combination of a baseline correction to deal with fluorescence along with comparatively small Raman signals can often make the fringing very apparent. The first example presented here is a bit different and involves rather strong Raman peaks as well as photoluminescence instead of fluorescence but the effects on the spectra are similar. Photoluminescence in silicon arises from defects and impurities and has been used to characterize a number of different types of silicon materials. Using a 805 nm excitation laser a photoluminescence peak has been reported centered near 1.10 eV (1127 nm) but the peak is broad and extends past 1.2 eV (1033 nm).[2] It seems likely that a shoulder associated with this peak may be observed in the higher shifted region of Raman spectra of silicon when using longer wavelength lasers such as 780 nm and 785 nm lasers. Figure 4 compares Raman spectra obtained from the same silicon sample using a 785 nm excitation laser on two different Raman imaging microscopes, one with a back illuminated (EM-CCD) detector and one with a front illuminated (CCD) detector. In both cases, the photoluminescence contribution is visible at higher shift values but the data from the back illuminated EM-CCD also shows the periodic (sine wave-like) features indicative of fringing. Using a 532 nm laser instead of the 785 nm laser not only avoids the photoluminescence peaks (out of the observed spectral range) but also would not show the issue with the fringing because of the lower penetration through the EM-CCD detector by the shorter wavelengths of light. Although here the fringing effect is located well away from the analytical silicon peak, in many cases the high shift region is critical, such as with a very thin coating of an organic material on a silicon substrate.

The next example involves a sample that exhibits weaker Raman peaks and fluorescence. Figure 5 shows Raman results obtained from ink on a 10 Euro note using 785 nm excitation. In both cases the raw spectra showed a significant baseline distortion due to fluorescence and the spectra shown in Figure 5 have been baseline corrected. Similar to the silicon data, the majority of the fingerprint region is not significantly affected by the fringing seen with the back illuminated EM-CCD system, but the higher shifted regions of the spectrum are significantly impacted. Having the fringing effects makes identifying peaks in the higher shift regions more difficult as well as detracting from the esthetic appearance of the spectrum.

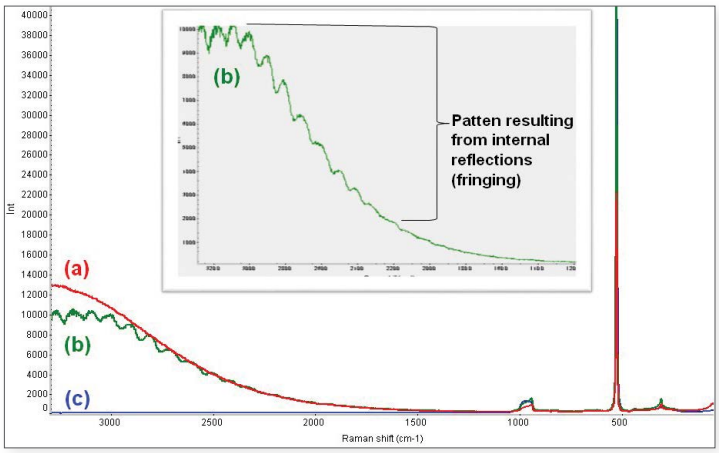

Figure 4: Raman spectra from a silicon sample, (a) spectrum obtained using a 785 nm laser with a DXR3 Raman Microscope using a front illuminated CCD detector (photoluminescence but no fringing), (b) spectrum obtained using a 785 nm laser with a DXR3xi Raman Imaging Microscope using a back illuminated EM-CCD detector (photoluminescence + fringing), (c) spectrum obtained using a 532 nm laser with a DXR3xi Raman Imaging Microscope using a back illuminated EM-CCD detector (no photoluminescence and no fringing). Insert is an expanded view of spectrum (b).

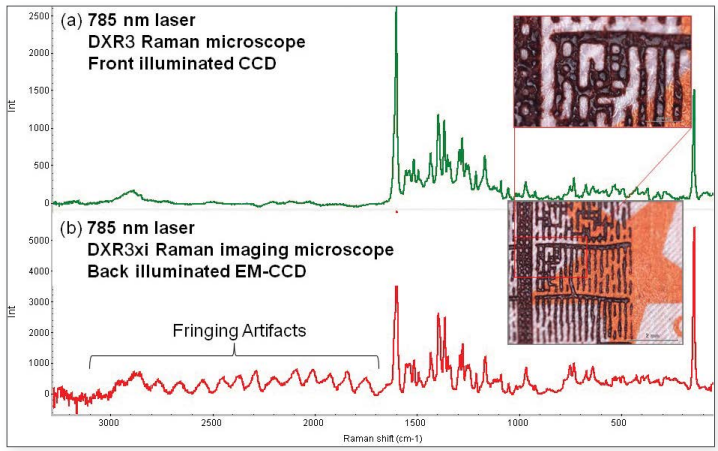

Figure 5: Raman spectra from ink used on a 10 Euro note. Both spectra have been baseline corrected to remove fluorescence contributions. (a) Spectrum obtained with a 785 nm laser in a DXR3 Raman Microscope using a front illuminated CCD detector does not show fringing. (b) Spectrum obtained with a 785 nm laser in a DXR3xi Raman Imaging Microscope using a back illuminated EM-CCD detector shows fringing artifacts.

Fringing becomes even more pronounced as the relative fluorescence contributions increase. Hair samples can show very little or extreme fluorescence depending on the nature of the hair sample being analyzed. The Raman spectrum of a hair with a moderate fluorescence contribution is shown in Figure 6. Again the spectra were collected using the back illuminated EM-CCD and the front illuminated CCD detector with 785 nm excitation. The spectra have been baseline corrected. The relative effect of the fringing is much greater in this spectrum and extends down near the fingerprint region. The Raman analysis of hair is challenging under the best conditions, so fringing further complicates the analysis. Despite the advantages in quantum efficiency the use of a back illuminated EM-CCD, in this case, can actually hinder the analysis.

A clear illustration of the QE versus fringing balance is shown in Figure 7. Spectra from imaging data collected on DXR3xi Raman Imaging Microscopes using 780 nm excitation and either a back illuminated or a front illuminated EM-CCD are compared. The spectra have been baseline corrected. The fringing intensity in the spectrum obtained using the back illuminated EM-CCD is clearly evident, but the spectrum has better signal to noise (about 1.6 times better) than the one using the front illuminated EM-CCD. The spectra from the front illuminated EM-CCD are a bit noisier, but show no fringing artifacts. So the choice here is between better signal to noise and fringing artifacts or lower signal to noise and no fringing. The difference is that longer exposure times can improve the signal to noise where the fringing artifacts cannot be removed by just altering the collection parameters.

That would seem to make a good case for using a front illuminated EM-CCD detector for Raman imaging, especially if you are dealing with long wavelength lasers and samples that fluoresce. However, there is a clear balance between fringing and the lower QE of the front illumination. The higher QE of back illumination is secondary if your samples display major fringing artifacts, but the lower QE does affect the signal to noise and may require longer exposure times to get acceptable spectral quality. Table 1 contains results from 4 different types of samples imaged with either the front illuminated or back illuminated EM-CCD. The silicon target was analyzed with both 532 nm and 785 nm excitation while the other samples were imaged using just the 532 nm laser. The Raman images themselves are similar for both detection schemes, but there is a significant difference in the signal to noise of the individual spectra. The tabulated values resulted from averages over similar regions in the data sets using the same overall collection parameters. In general the signal to noise using the front illuminated detector was about half of that obtained using the back illuminated detector. This corresponds well to the difference in the QE of the detectors, showing the potential reduction in signal to noise when using a front illuminated EM-CCD.

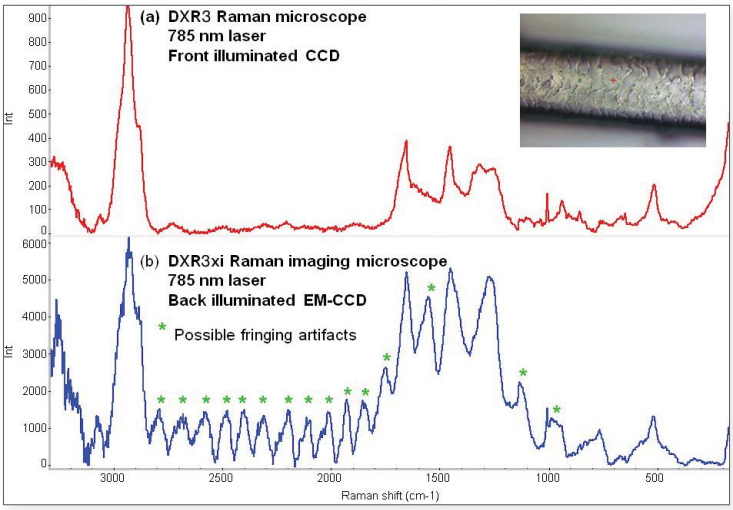

Figure 6: Raman spectra from a human hair sample. Both spectra have been baseline corrected to remove fluorescence contributions. (a) Spectrum obtained with a 785 nm laser in a DXR3 Raman Microscope using a front illuminated CCD detector does not show fringing. (b) Spectrum obtained with a 785 nm laser in a DXR3xi Raman imaging microscope using a back illuminated EM-CCD detector shows significant fringing artifacts.

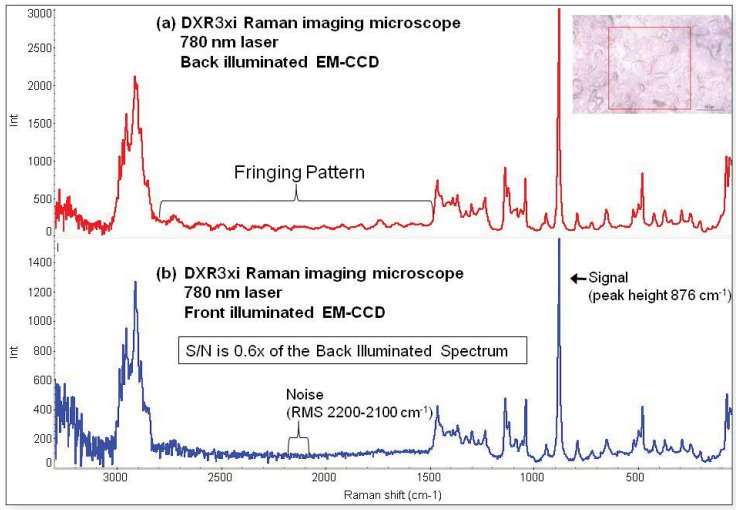

Figure 7: Raman spectra of Mannitol containing regions of a sample. Both spectra have been baseline corrected to remove fluorescence contributions. (a) Spectrum obtained with a 780 nm laser in a DXR3xi Raman Imaging Microscope using a back illuminated EM-CCD detector shows significant fringing artifacts. (b) Spectrum obtained with a 780 nm laser in a DXR3xi Raman Imaging Microscope using a front illuminated EM-CCD detector shows no fringing artifacts.

thermo scientific

Sample	Laser	Exposure time (s)	Relative S/N ratios (S/N front illuminated EM-CCD / S/N back illuminated EM-CCD)
Silicon target	532 nm	0.00174	0.43
Silicon target	785 nm	0.00200	0.48
Graphene on Si (2D peak)	532 nm	0.00200	0.40
Pyrite (mineral)	532 nm	0.01000	0.46
Tablet (Aspirin)	532 nm	0.00250	0.62

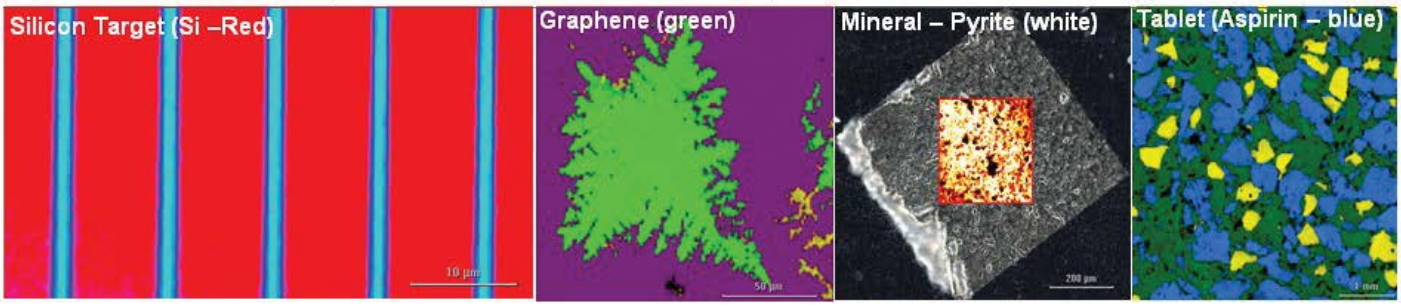

Table 1: The effect that differences in quantum efficiency can have on imaging data. Raman spectral data from 4 different Raman imaging samples (a silicon target, mono-layer graphene on silicon, a Pyrite deposit in a mineral sample, and Aspirin in a tablet sample) show how the difference in quantum efficiency translates into differences in signal-to-noise ratios.

Conclusion

We have seen some examples that illustrate the trade-off between fringing and quantum efficiency (characterized by signal to noise) of CCD-based imaging sensors in front and back illuminated modes. Table 2 summarizes when it is advantageous to use one type of CCD detector over the other.

The choice of the right technology depends on the nature of the samples being analyzed and the application requirements. The ideas presented in this paper should be considered when assessing what technology provides the best choice to achieve these goals.

References

1. *Comparing the Performance of EM-CCD and CCD Cameras for Raman Microscope Applications*, Robert Heintz, WP52981, Thermo Fisher Scientific, 2017.

2. S. Binetti, A. Le Donne, M. Acciarri, Solar Energy Materials & Solar Cells, **86** (2005) 11–18

	Back illuminated EM-CCD	Front illuminated EM-CCD
Raman analysis using short wavelength lasers (Example: 532 nm)	**Preferred**	Lower S/N no benefit
Raman analysis requiring long wavelength lasers (Examples: 780 nm , 785 nm)	Might see fringing artifacts (especially if samples still show fluorescence)	**Preferred**
Raman Imaging where fastest speed is essential	**Preferred** (higher QE)	Not ideal unless the samples require a long wavelength laser
Samples that require long exposure times and long wavelength lasers – weak Raman signals and significant fluorescence (biological samples, inks, etc.)	Fringing artifacts will be a major issue	**Preferred**

Table 2: Best choice of CCD detector types based on samples and application requirements.

Find out more at **thermofisher.com/Raman**

ThermoFisher SCIENTIFIC